High-intensity molecular harmonic generation without ionization*

Wang Jun(王 俊)[a], Chen Gao(陈 高)[b], Guo Fu-Ming(郭福明)[a], Li Su-Yu(李苏宇)[a], Chen Ji-Gen(陈基根)[c], and Yang Yu-Jun(杨玉军)[a]†

[a] *Institute of Atomic and Molecular Physics, Jilin University, Changchun* 130012, *China*
[b] *School of Science, Changchun University of Science and Technology, Changchun* 130022, *China*
[c] *Department of Physics and Materials Engineering, Taizhou University, Taizhou* 318000, *China*

(Received 1 November 2012; revised manuscript received 19 December 2012)

We theoretically investigate high-order harmonic generation from H_2^+ in an infrared laser field. Our numerical simulations show that a highly efficient plateau structure exists in the molecular harmonic spectrum. Under the action of the infrared laser pulse, the bound electronic wave packet in a potential well has enough time to tunnel through the effective potential barrier, which is formed by the molecular potential and the infrared laser field, and then recombine with the neighboring nucleus emitting a harmonic photon. During the entire dynamic process, because the wave packet is mainly located in the effective potential, the diffusion effect is of no significance, and thus a highly efficient harmonic plateau can be achieved. Specifically, the cut-off frequency of the plateau is linearly scaled with the peak amplitude of the infrared laser electric field, which may open another route to examine the internuclear distance of the molecule. Furthermore, one may detect the molecular bond lengths using the harmonic plateau.

Keywords: molecular harmonic, bond lengths, diagnosis

PACS: 32.80.Rm, 42.50.Hz **DOI:** 10.1088/1674-1056/22/3/033203

1. Introduction

The interaction of an intense laser pulse with atomic and molecular systems results in high-order harmonic generation (HHG). Because the HHG spectrum owns an apparent plateau structure, i.e., with the increase of the harmonic order, many harmonics have nearly the same intensity. Therefore, HHG becomes a potential tunable coherent light source ranging from XVU to soft X-ray, and an important scheme to generate an isolated attosecond pulse.[1–5]

When atoms are irradiated by a linearly polarized laser pulse, the HHG mechanism can be well understood in terms of the semi-classical three-step model.[6,7] The electron first tunnels through the effective potential barrier formed by the atom and the laser field, then oscillates in the field, and finally may recombine with the ground state and emit a harmonic photon with energy equal to the ionization potential plus the kinetic energy of the recombining electron. The maximal photon energy can be predicted by the cut-off rule, $I_p + 3.17U_p$, where I_p is the atomic ionization energy, and $U_p = E_0/4\omega^2$ is the ponderomotive energy of the laser field, with E_0 and ω being the peak amplitude and frequency of the incident laser field, respectively.

For the molecular HHG spectrum, due to the multicenter structure of the molecule, an evident interference structure exists, and the vibration and rotation of the molecule also have an effect on the HHG. Furthermore, the orbital energy of the molecule is closer than that of the atomic gas medium. Thus, the molecular HHG can be applied to reconstruct molecular orbits, detect the dynamics of molecular vibration and rotation, and probe the electronic dynamics of the molecules on an ultrashort time scale.[8–16]

However, the conversion efficiency of the HHG is usually low because of the small ionization probability and the diffusion effect of the ionized electronic wave packet in the laser pulse. Therefore, researchers are interested in enhancing the HHG intensity. [17–19] The improvement of harmonic conversion efficiency has been studied by preparing the initial state as a coherent superposition of two bound states and using combined pulses.[20–23] Owing to the multi-atomic center structure in the molecule, the bound electron driven by an intense laser field can move from an atomic center to another one without ionization. In this way, one can achieve HHG with a higher efficiency. Significantly, it is found that a HHG with higher efficiency is generated as the potential energy difference between the two nuclei is equal to $\boldsymbol{E}(t)\cdot\boldsymbol{R}$. It can be applied to detect the molecular bond lengths. In this paper, we explore this mechanism to generate highly efficient harmonics of the molecule exposed in the infrared laser pulse. Atomic unit (a.u.) is adopted in this paper, unless specially stated.

2. Theory

In this paper, we pay no attention to the molecular alignment and orientation effect. Therefore, the molecular HHG

*Project supported by the National Basic Research Program of China (Grant No. 2013CB922200), the National Natural Science Foundation of China (Grant Nos. 11274141 and 11034003), and the Natural Science Foundation of Zhejiang Province, China (Grant No. Y6110578).

†Corresponding author. E-mail: yangyj@jlu.edu.cn

© 2013 Chinese Physical Society and IOP Publishing Ltd

can be logically investigated by a one-dimensional (1D) or two-dimensional (2D) model.[24–28] The molecular axis is restricted along the polarization direction of the linearly polarized laser pulse. In the dipole approximation and length gauge, the 2D time-dependent Schrödinger equation is given by

$$\mathrm{i}\frac{\partial\psi(x,y,t)}{\partial t} = H(x,y,R,t)\psi(x,y,t), \tag{1}$$

where

$$H(x,y,R,t) = -\frac{1}{2}\frac{\partial^2}{\partial x^2} - \frac{1}{2}\frac{\partial^2}{\partial y^2} + V_{\mathrm{c}}(x,y,R) - xE(t), \tag{2}$$

with R being the internuclear distance of the molecule. In our calculation, the soft Coulomb potential is adopted

$$\begin{aligned} V_{\mathrm{C}}(x,y,R) \;=\; & -Z/\sqrt{(x-R/2)^2+y^2+a} \\ & - Z/\sqrt{(x+R/2)^2+y^2+a}, \end{aligned} \tag{3}$$

where a is the soft-core parameter. We set $a = 0.61$ and $R = 7$, so that the energy of the ground electronic state of the 2D model (-0.519 a.u., including the $1/R$ nuclear repulsion) and we can reproduce the value for the actual H_2^+ in 3D space. The $E(t)$ is the electric field of the linearly polarized laser pulse,

$$E(t) = E_0 f(t)\sin(\omega_0 t), \tag{4}$$

where E_0 and ω_0 are the peak amplitude and frequency of the laser electric field, respectively. The envelope function pulse is Gaussian-type: $f(t) = \exp[-4\ln 2(t/\sigma)^2]$. The TDSE can be efficiently solved by means of the well-known split-operator method.[29] Once the wave function at any moment $\psi(x,y,t)$ is obtained, the time-dependent induced dipole acceleration can be given by means of Ehrenfest's theorem as follows:

$$a(t) = -\left\langle \psi(x,y,t) \left| \frac{\mathrm{d}V_{\mathrm{c}}(x,y,R)}{\mathrm{d}x} - E(t) \right| \psi(x,y,t) \right\rangle. \tag{5}$$

The HHG power spectrum is proportional to the modulus squared of the Fourier transform of $a(t)$. It is given by

$$P(\omega) = \left| \frac{1}{\sqrt{2\pi}} \int_0^t a(t)\,\mathrm{e}^{-\mathrm{i}\omega t}\,\mathrm{d}t \right|^2. \tag{6}$$

In order to study the detailed spectral and temporal structures of HHG, we perform time-frequency analysis by means of the wavelet transform

$$A_\omega(t_0,\omega_0) = \int_{t_{\mathrm{i}}}^{t_{\mathrm{f}}} a(t) W_{t_0,\omega}(t)\,\mathrm{d}t. \tag{7}$$

For the harmonic emission, a natural choice of the mother wavelet is given by the Morlet wavelet

$$W(x) = \frac{1}{\sqrt{\tau}}\,\mathrm{e}^{\mathrm{i}x}\,\mathrm{e}^{-x^2/2\tau^2}. \tag{8}$$

In order to investigate the mechanism of the high efficient harmonic generation, we separate the time-dependent-induced dipole acceleration into two parts in space,

$$a(t) = a_{x>0}(t) + a_{x<0}(t). \tag{9}$$

3. Results and discussion

We first investigate the high-order harmonic generation process from H_2^+ driven by an infrared laser pulse with a wavelength of 3200 nm. The inset in Fig. 1 shows the HHG spectrum from H_2^+ in the infrared laser pulse. Here, the peak electric amplitude of the infrared laser pulse is $E_0 = 0.03$, and the duration is 3 optical cycles. Note that an available few-cycle intense laser pulse with a wavelength from 1 μm to 5 μm can be achieved by the optical parametric amplification technology. The harmonic spectrum shows a plateau structure and ends up at around the 295th order, which agrees well with the prediction of the semi-classical three-step model. It is worth noting that there is an additional plateau with high intensity in the low order part of the harmonic spectrum, as presented in Fig. 1. In comparison with the plateau in the high order part of the HHG, its conversion efficiency is enhanced by about 9 orders of magnitude.

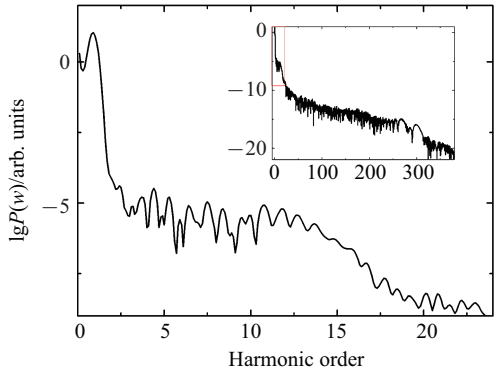


Fig. 1. Highly efficient harmonic spectrum generated from the laser field with a peak amplitude of $E_0 = 0.03$ and a wavelength of 3200 nm. The whole harmonic spectrum is shown in the inset.

In order to study the mechanism of highly efficient harmonic generation, we changed the intensity of the incident laser field. Figures 2(a)–2(c) show harmonic spectra with different peak amplitudes $E_0 = 0.01$, 0.02, and 0.03, and cut-off orders of the highly efficient harmonic spectra are the 5th, 10th, and 15th, respectively. It can be seen that the cut-off frequency of the high efficient plateau increases gradually with the peak amplitude of the laser field. In particular, the cut-off energy of the highly efficient harmonic is in proportion to the peak amplitude of the electric field. This does not obey the cut-off law of high-energy harmonic generation: $E_{\mathrm{cut-off}} = I_{\mathrm{p}} + 3.2U_{\mathrm{p}}$, which clearly states that the cut-off energy increases with the peak intensity of the laser field. In the same peak intensity, by changing the frequency of the laser field, we found that the cutoff energy will not change with the variation of frequency in a certain frequency range.

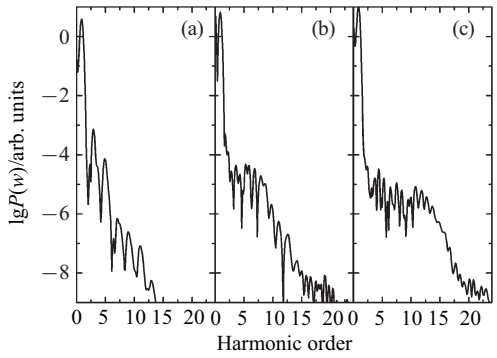


Fig. 2. High-order harmonic spectra from H_2^+ subject to the laser field with different peak amplitudes (a) $E_0 = 0.01$, (b) $E_0 = 0.02$, and (c) $E_0 = 0.03$.

Figure 3 shows the dependence of the cut-off order of the highly efficient plateau on the peak electric amplitude E_0 of the incident laser pulse, which ranges from 0.01 to 0.04. This figure also presents the E_0 dependence of the function E_0R. One can see that the two curves are almost the same. This result further demonstrates that the cut-off frequency of the highly efficient plateau is proportional to the peak electric amplitude E_0, and the scale factor is the internuclear distance of the molecule. To verify the relationship between the molecular potential function and the highly efficient plateau, we also changed the internuclear distance R, and found that the cut-off frequency of the highly efficient plateau has a direct ratio with R.

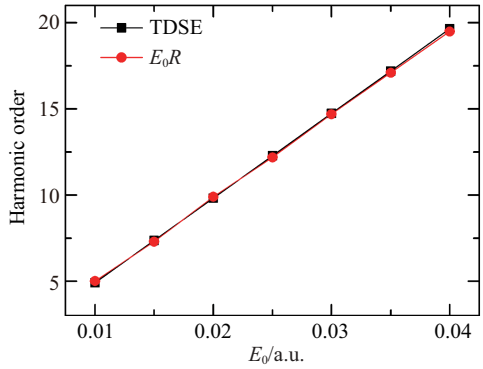


Fig. 3. (color online) Relationship between the cut-off order of highly efficient harmonics and the peak amplitude of the incident laser field.

In order to explore the mechanism of highly efficient harmonic generation, the time-dependent dipole acceleration is divided into the positive $a_{x>0}(t)$ and the negative $a_{x<0}(t)$ parts, as shown in Eq. (8). Because the harmonic emission is a local profile center around the potential center, we can independently analyze the contribution of the two atomic nuclei by using the two time-dependent dipole accelerations. Figure 4(a) shows the electric field of the driving laser pulse. Figure 4(b) presents the positive and negative time-dependent dipole accelerations. One can observe that the time-dependent change of the behavior of $a_{x<0}(t)$ is very similar to that of $a_{x>0}(t)$, but a difference still exists in two cases: the quick oscillations appear at the moments of about 564 and 758 (corresponding to the first and second peak of the laser field) for the two cases of $a_{x>0}(t)$ and $a_{x<0}(t)$, respectively. Figures 4(c) and 4(d) depict the time frequency analysis of the positive and negative dipole acceleration, respectively. One can see that the main emission region of the highly efficient harmonics is near the peak of the electric field, which is different from the case of the harmonics generated by tunneling ionization. The main regions of the harmonic emission occur at the moments 564 and 758 for $a_{x>0}(t)$ and $a_{x<0}(t)$, respectively. These results from the time-frequency analysis are consistent with those shown by the positive and negative dipole.

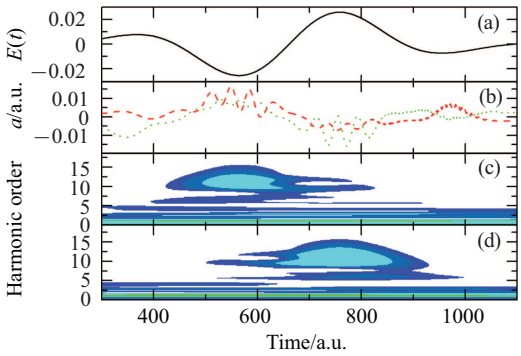


Fig. 4. (color online) (a) Laser field of the driving pulse; (b) time-dependent dipole acceleration $a_{x<0}(t)$ (dotted green curve) and $a_{x>0}(t)$ (dashed red curve); (c) and (d) shows the time-frequency analysis of $a_{x<0}(t)$ and $a_{x>0}(t)$, respectively.

From the emission time profile analysis, we noticed that the highly efficient harmonic generation cannot be interpreted by the three-step model. In addition, these harmonics cannot be generated by the transition between the bound states, because the cut-off frequency of the highly efficient plateau changes with the peak amplitude of the laser electric field. On the other hand, we cannot observe a similar high efficient harmonic from atoms irradiated by the same laser pulse. Thus harmonic generation should be generated by the scattering of the bound electron with another nucleus of the molecule.

The mechanism can be illustrated using the sketch map of Fig. 5. The dashed red and solid black curves in Fig. 5 denote the probability density of the initial state and the molecular potential function, respectively. The two centers of the molecular potential well are labeled as A and B. When the laser electric field is applied, the potential is strongly distorted, as shown by the dash-dotted blue curve in Fig. 5. Here, we would like to point out that the incident laser pulse we used is a mid-infrared one, which keeps almost the same potential barrier in a certain time regime, and the bound electronic wave packet in potential well A has enough time to tunnel the potential barrier between the two wells and scatter with nuclear B, as shown by the dotted green curve in Fig. 5. In this dynamic process, there is no obvious diffusion effect of the electronic wave packet, which

is mainly located in the distorted potential. Therefore, high efficient harmonics can be produced.

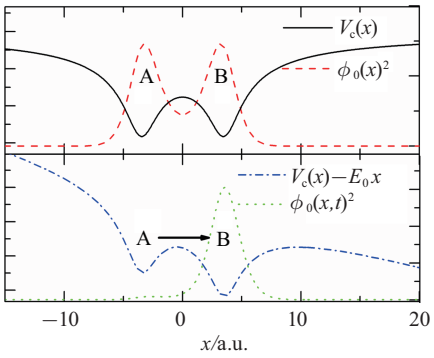


Fig. 5. (color online) Sketch map of the mechanism of highly intense harmonic generation. Solid black curve: the potential barrier; dash-dotted blue curve: the effective potential barrier formed by the molecule and the laser field; dashed red curve: the square of the initial wave function; dotted green curve: the square of the wave function of the system for the maximum electric field intensity.

When the wave packet tunnels through the effective potential barrier from A to B, it can be accelerated by the electric field, and the kinetic energy with $\boldsymbol{E}(t)\cdot\boldsymbol{R}$ can be obtained. From the aspect of the quantum transition, the electron originally stays in the ground-state of potential well A and B. The laser field depresses the potential barrier B, and raises the potential barrier A, resulting in the split of the initial energy level to the upper and lower levels, and the energy difference of which is $\boldsymbol{E}(t)\cdot\boldsymbol{R}$. When the wave packet moves from A to B scattering with the B, and the electron transits from the upper level to the lower one induced by the field accompanying the emission of the photon, the energy of which is $\boldsymbol{E}(t)\cdot\boldsymbol{R}$.

It should be pointed out that the mechanism is more obvious to the mid-infrared laser field, because the electron has enough time to penetrate the potential barrier in the middle of the two potential wells, thus the high efficient harmonic emission can be generated. In the experiments, the molecule can first be aligned and dissociated by an appropriate pre-pulse. By controlling the time delay between the pump pulse and the driving laser, the aligned molecule with a suitable distance between the two nuclei can be obtained, and then the highly efficient harmonics can be generated by an intense mid-infrared laser pulse. As a result, based on this HHG, isolated attosecond pulses with a high intensity can be generated. Moreover, one can detect the internuclear distance of the molecule because the cut-off order of the high efficient plateau equals $\boldsymbol{E}(t)\cdot\boldsymbol{R}$. Specifically, due to the multiple centers in the crystal, it can act as a reference for the HHG research in the crystal.

4. Conclusion

In conclusion, high-order harmonic generation from the molecule irradiated by the mid-infrared laser pulse is investigated, and we find a highly efficient plateau in the leading part of the harmonic spectrum (the conversion efficiency of which can be improved by 9 orders of magnitude compared to that of the harmonic generated by the ionized electron recombining with the ground state). The cut-off energy of the highly efficient harmonic generation is in proportion to the peak amplitude of the incident laser field and the internuclear distance of the molecule. This plateau can be used as a tool to detect the instant bound length of molecules in the strong laser field.

Acknowledgments

The authors are grateful to Professor Jing Chen for helpful discussion. We acknowledge the High Performance Computing Center of Jilin University for supercomputer time.

References

[1] McPherson A, Gibson G, Jara U, Johann H, Luk T S, McIntyre I A, Boyer K and Rhodes C K J 1987 *Opt. Soc. Am. B* **4** 595
[2] Miyazaki K, Kaku M, Miyaji G, Abdurrouf A and Faisal F H M 2005 *Phys. Rev. Lett.* **95** 243903
[3] Spielmann Ch, Burnett N H, Sartania S, Koppitsch R, Kan C, Lenzner M, Wobrauschek P and Krausz F 1997 *Science* **278** 661
[4] Paul P M, Toma E S, Breger P, Mullot G, Auge F, Balcou P, Muller H G and Agostini P 2001 *Science* **292** 1689
[5] Chen J G, Li C, Chi F P and Yang Y J 2007 *Chin. Phys. Lett.* **24** 86
[6] Corkum P B 1993 *Phys. Rev. Lett.* **71** 1994
[7] Lewenstein M, Balcou P, Ivanov M Y, L'Huillier A and Corkum P B 1994 *Phys. Rev. A* **49** 2117
[8] Itatani J, Levesue J, Zeidler D, Niikura H, Pépin H, Kieffer J C, Corkum P B and Villeneuve D M 2004 *Nature* **432** 867
[9] Lein M 2005 *Phys. Rev. Lett.* **94** 053004
[10] Ramakrishna S and Seideman T 2007 *Phys. Rev. Lett.* **99** 113901
[11] McFarland B K, Farrell J P, Bucksbaum P H and Gühr M 2008 *Science* **332** 1232
[12] Wörner H J, Bertrand J B, Kartasho D V, Corkum P B and Villeneuve D M 2010 *Nature* **446** 604
[13] Lock R M, Ramakrishna S, Zhou X, Kapteyn H C, Murnane M M and Seideman T 2012 *Phys. Rev. Lett.* **108** 133901
[14] Zwan E V and Lein M 2012 *Phys. Rev. Lett.* **108** 043004
[15] Lein M, Hay N, Velotta R, Marangos J P and Knight P L 2002 *Phys. Rev. A* **66** 023805
[16] Wang B B, Li X F and Fu P M 1998 *Chin. Phys. Lett.* **15** 195
[17] Sansone G, Benedetti E, Caleari F, Vozzi C, Avaldi L, Flammini R, Poletto L, Villoresi P, Altucci C, Velotta R, Stagira S, Silvestri S and Nisoli M 2006 *Science* **314** 443
[18] Goulielmakis E, Schultze M, Fstetter M, Yakovlev V S, Garnon J, Uiberacker M, Aquila A L, Gullikson E M, Attwood D T, Kienberger R, Krausz F and Kleineberg U 2008 *Science* **320** 1614
[19] Chen J G, Yang Y J, Zeng S L and Liang H Q 2011 *Phys. Rev. A* **83** 023401
[20] Chen G, Chen J G, Yang Y J, Zhu H Y, Du W H, Chi F P and Zhu Q R 2005 *Chin. Phys. Lett.* **22** 584
[21] Sanpera A, Watson J B, Lewenstein M and Burnett K 1996 *Phys. Rev. A* **54** 4320
[22] Ishikawa K 2003 *Phys. Rev. Lett.* **91** 043002
[23] Wang B B, Cheng T W, Li X F, Fu P M, Chen S and Liu J 2005 *Phys. Rev. A* **72** 063412
[24] Lein M, Hay N, Velotta R, Marangos J P and Knight P L 2002 *Phys. Rev. A* **66** 023805
[25] Person E, Burgdorfer J and Grafe S 2009 *New J. Phys.* **11** 105035
[26] Yang Y J, Chen J G, Chen G and Zhu Q R 2004 *Chin. Phys. Lett.* **21** 652
[27] Zhao J and Zhao Z X 2010 *Chin. Phys. Lett.* **27** 063301
[28] Takemoto N and Becker A 2011 *J. Chem. Phys.* **134** 074309
[29] Yang Y J, Chen J G, Chi F P, Zhu Q R, Zhang H X and Sun J Z 2007 *Chin. Phys. Lett.* **24** 1537